Supporting Information:

InP Quantum Dots: An Environment Friendly Material with Resonance Energy Transfer Requisites

Anoop Thomas, Pratheesh V. Nair and K. George Thomas*

School of Chemistry, Indian Institute of Science Education and Research Thiruvananthapuram (IISER-TVM), CET Campus, Thiruvananthapuram, 695 016, India

Table of contents

1. Synthesis of InP/ZnS quantum dots

Myristic acid capped InP QDs were synthesized by following a reported procedure with minor modifications.[1] Indium acetate (0.4 mmol, 0.112 g) and myristic acid (1.54 mmol, 0.35g) in octadecene (5 mL) was heated to 120 ^{o}C in a three necked round bottom flask equipped with a thermometer under nitrogen atmosphere and a clear solution was obtained. The reaction vessel containing above solution was evacuated for 30 min keeping the temperature at 120 ^{0}C and the further raised to 200 ^{o}C under inert atmosphere. Maintaining the temperature at 200 ^{0}C, a solution of tris(trimethylsilylphosphine) (0.2 mmol, 58 μL) and octylamine (2.4 mmol, 400 μL) in octadecene (1 mL) was injected which results in the formation of InP quantum dots. Once the desired size was obtained, the crystal growth was arrested by reducing the reaction temperature to 130 ^{o}C. An aliquot was withdrawn from the solution and purified by precipitation from a mixture (4:1) of acetone and methanol, followed by centrifugation yielded bare InP QDs. QDs were further overcoated with ZnS in the same reaction vessel. A mixture of diethylzinc (684 μL, 1 M solution in hexane) and hexamethyldisilathiane (128 μL) in octadecene (2 mL), required for overcoating three monolayers of ZnS over InP was slowly injected into the reaction mixture over a period of 30 min. After the injection is complete, the temperature was raised to 200 ^{o}C and stirring was continued for 2 h which resulted in the growth of ZnS shell. The InP/ZnS QDs were added to cold hexane (5 ^{o}C) to arrest further growth of the shell. Overcoated samples (InP/ZnS) were purified by precipitation from a mixture (4:1) of acetone and methanol, followed by centrifugation. The residue was redispersed in hexane and the purification procedure was repeated thrice and stored in chloroform further studies.

2. Steady state absorption and emission of InP quantum dots

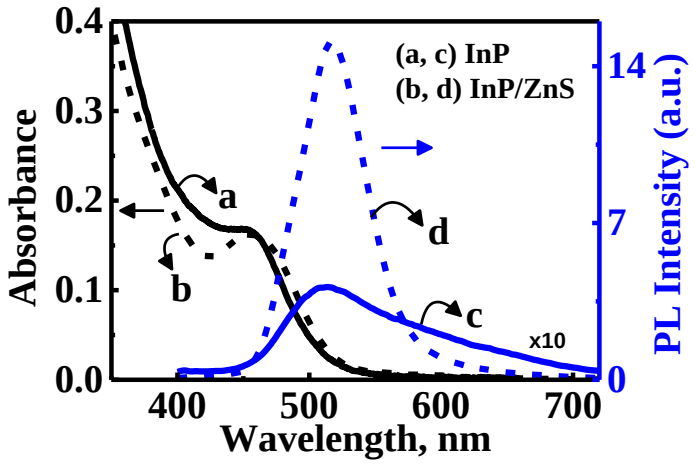

Figure S1. Absorption spectra of InP (black solid trace a), InP/ZnS (black dashed trace b) quantum dots and the emission spectra of InP (blue solid trace c), InP/ZnS (blue dashed trace d). Emission spectrum of InP (trace c) is multiplied 10 times for comparison.

3. TEM Investigation

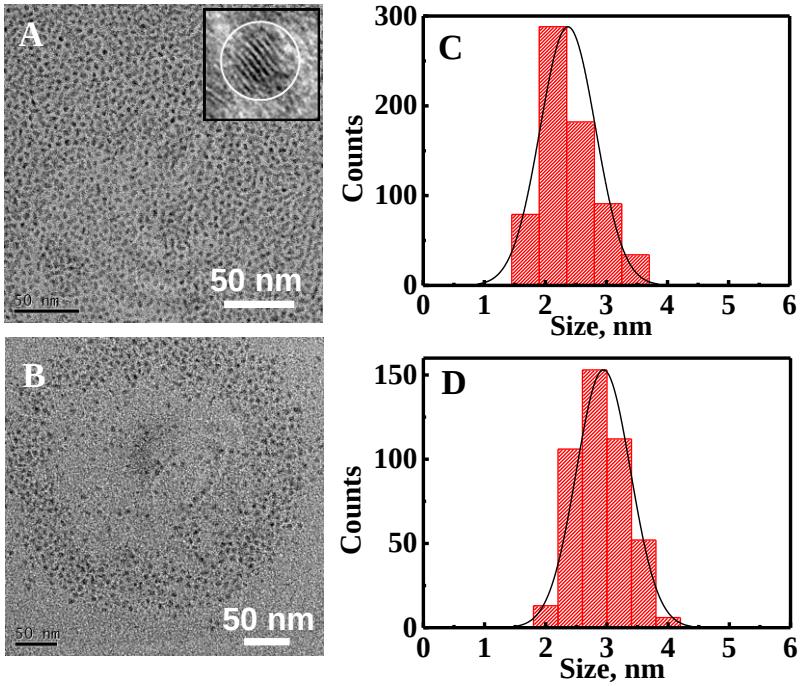

Figure S2. TEM images of (A) InP and (B) InP/ZnS quantum dots. The corresponding size histograms are given in C (InP) and D (InP/ZnS).

4. EDX Analysis of InP and InP/ZnS quantum dots

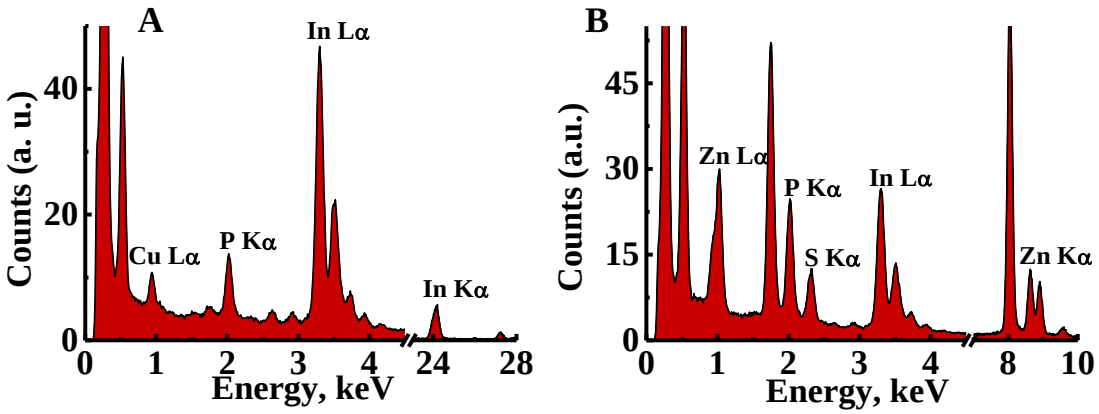

Figure S3. EDX spectrum of (A) InP and (B) InP/ZnS quantum dots.

Table S1. EDX energy values of component elements in InP and InP/ZnS QDs

Element	Energy value (keV)	
	Kα	Lα
In	24.209	3.296
P	2.014	-
Zn	8.632	1.02
S	2.301	-

5. Selective excitation of InP/ZnS

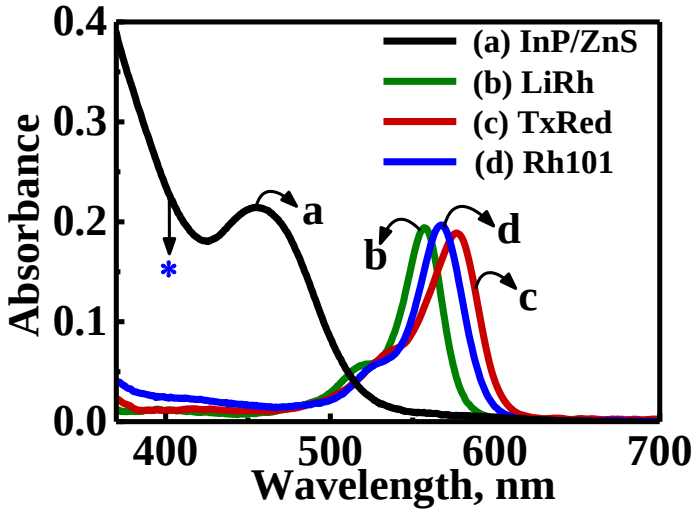

Figure S4. Absorption spectrum of InP/ZnS (black trace a), LiRh (green trace b), TxRed (red trace c) and Rh101 (blue trace d) in chloroform. The asterisk indicates the excitation wavelength (400 nm).

6. Emission properties of chromophoric dyes

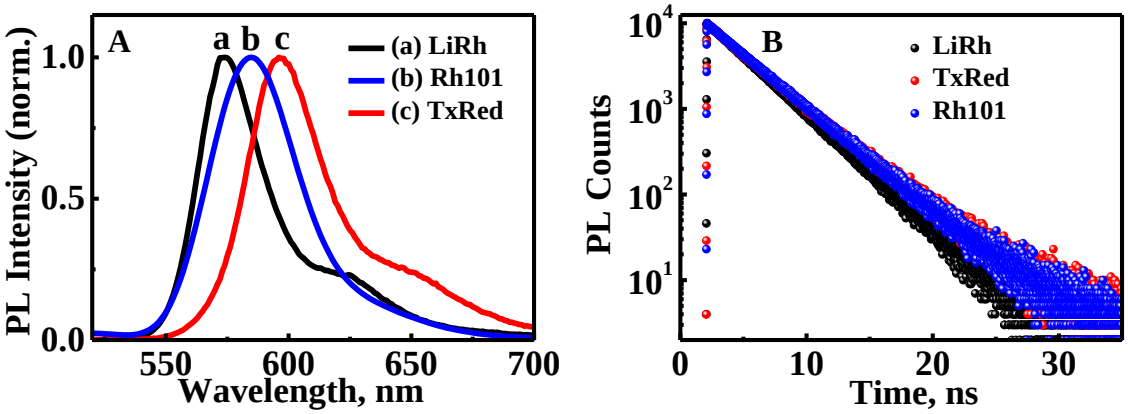

Figure S5. (A) Emission spectrum of LiRh (black trace a), Rh101 (blue trace b) and TxRed C5 (red trace c) in chloroform. (B) The fluorescence decay curves of the chromophoric dyes LiRh (black dots), TxRed C5 (red dots) and Rh101 (blue dots) on 405 nm excitation.

7. Absorption and emission of chromophoric dyes in the presence and absence of InP/ZnS QDs

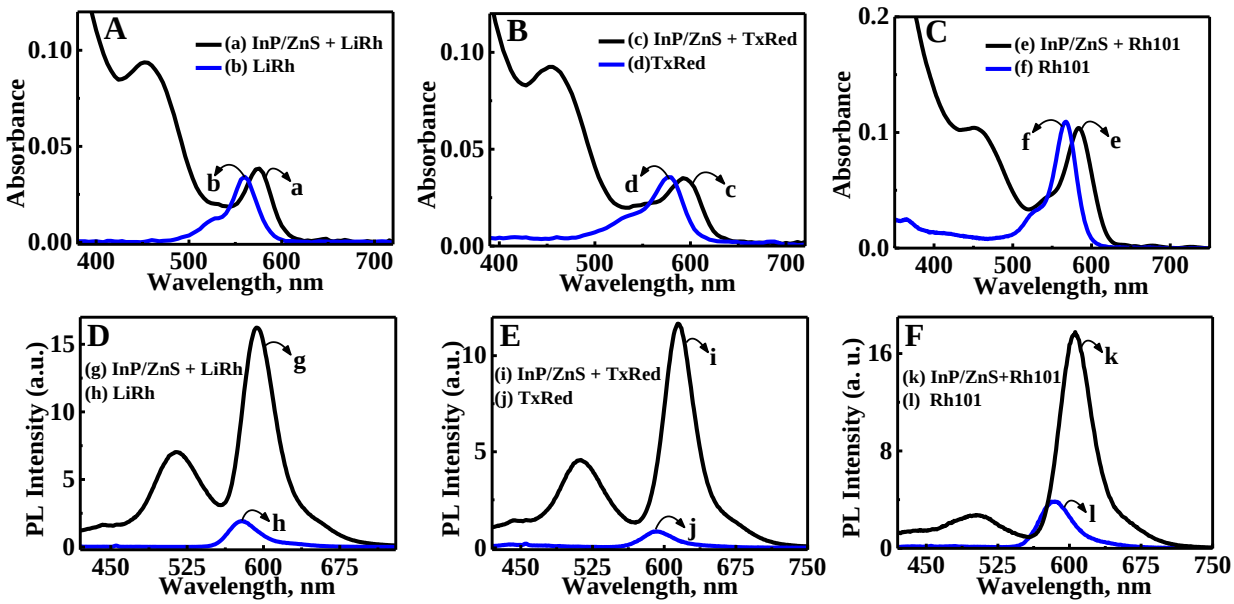

Figure S6. (A-C) Absorption spectrum of (A) LiRh (0.25 μM) in the presence (trace a) and absence (trace b) of InP/ZnS, (B) TxRed (0.40 μM) in the presence (trace c) and absence (trace d) of InP/ZnS, (C) Rh101 (1.0 μM) in the presence (trace e) and absence (trace f) of InP/ZnS. (D-F) Corresponding emission spectrum recorded by exciting at 400 nm (D) LiRh in the presence (trace g) and absence (trace h) of InP/ZnS, (E) TxRed in the presence (trace i) and absence (trace j) of InP/ZnS, (F) Rh101 in the presence (trace k) and absence (trace l) of InP/ZnS. All studies were carried out in chloroform.

The absorption and emission maxima of chromophoric dyes underwent a red shift of ~15 nm in the presence of InP/ZnS quantum dots compared to that of the free dyes indicating a strong interaction between the donor acceptor pair. In the presence and absence of InP/ZnS, the concentration of dye was kept constant and emission intensity of chromophoric dyes was found to be low in the absence of InP/ZnS.

8. Control experiments

Control experiments were carried out using a chromophoric dye molecule, Nile Red as an acceptor. Nile Red possesses very good spectral overlap with InP/ZnS emission.

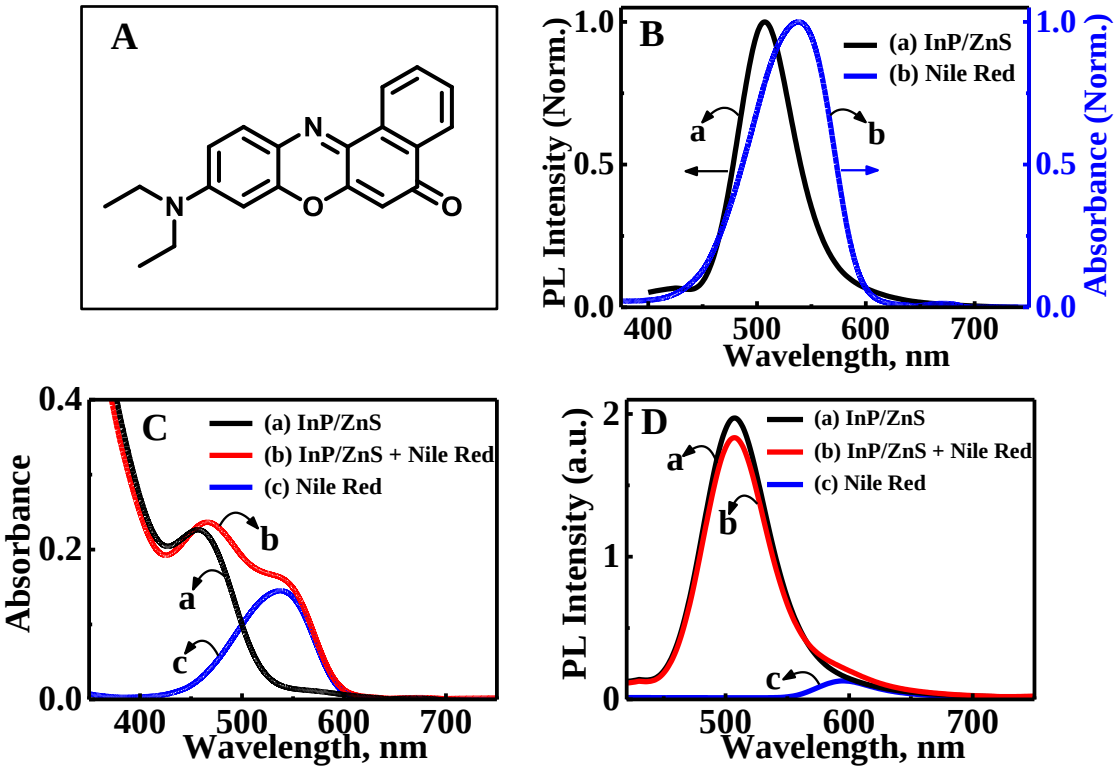

Figure S7. (A) Structure of Nile Red. (B) Emission of InP/ZnS quantum dot (black trace a) and Nile Red absorption (blue trace b) showing high spectral overlap. (C) Absorption spectrum of InP/ZnS in the absence (black trace a) and presence of Nile Red (3.84 μM, red trace b) and Nile Red (3.84 μM) in the absence of InP/ZnS (blue trace c). (D) Emission spectra of InP/ZnS quantum dots (black trace a) on addition of Nile Red (3.84 μM; red trace b) and Nile Red (3.84 μM) in the absence of InP/ZnS (blue trace c). All experiments were carried out in chloroform.

Absorption spectrum of InP/ZnS in the presence of Nile Red is an additive spectrum of individual components. The energy transfer from InP/ZnS to Nile Red was ruled out based on the following observation: (i) Emission corresponding to Nile Red was not observed on addition of InP/ZnS, (ii) growth corresponding to the formation of the excited state of Nile Red was not observed as in the case of LiRh, TxRed and Rh101.

9. Emission lifetime analysis

9.1. InP/ZnS emission decay analysis at long time scale

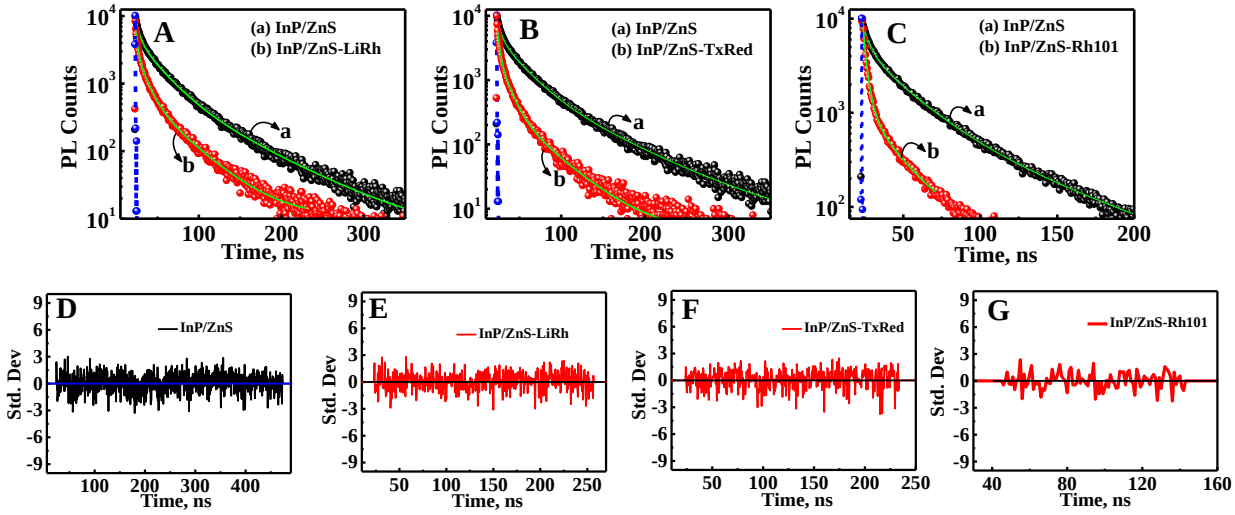

Figure S8. (A-C) Fitted luminescence decay profile of InP/ZnS in the absence (black trace a in A-C) and presence of chromophoric dye (represented by red trace b): (A) LiRh, (B) TxRed and (C) Rh101 monitored at 515 nm. The triexponential fit is represented by green solid line in (A-C). The blue dashed trace (A-C) is the lamp profile of the picosecond pulse. Residual plots showing the standard deviation of the triexponential fit are shown in (D-G); (D) InP/ZnS, (E) InP/ZnS-LiRh, (F) InP/ZnS-TxRed and (G) InP/ZnS-Rh101.

Table S2. Emission decay analysis of bare and chromophore bound InP/ZnS measured in a time window of 1 μs

Sample	τ_1(ns)	α_1	τ_2(ns)	α_2	τ_3(ns)	α_3	τ_{avg}(ns)	Chi. Sq
InP/ZnS	4.24	0.47	23.05	0.42	66.27	0.11	37.63	1.08
InP/ZnS-LiRh	1.03	0.54	5.46	0.33	23.32	0.13	15.07	1.13
InP/ZnS-TxRed	1.07	0.59	4.83	0.32	20.58	0.09	11.45	1.20
InP/ZnS-Rh101	1.11	0.52	3.11	0.32	15.82	0.16	10.08	1.20

9.2. Emission decay analysis at short time scale

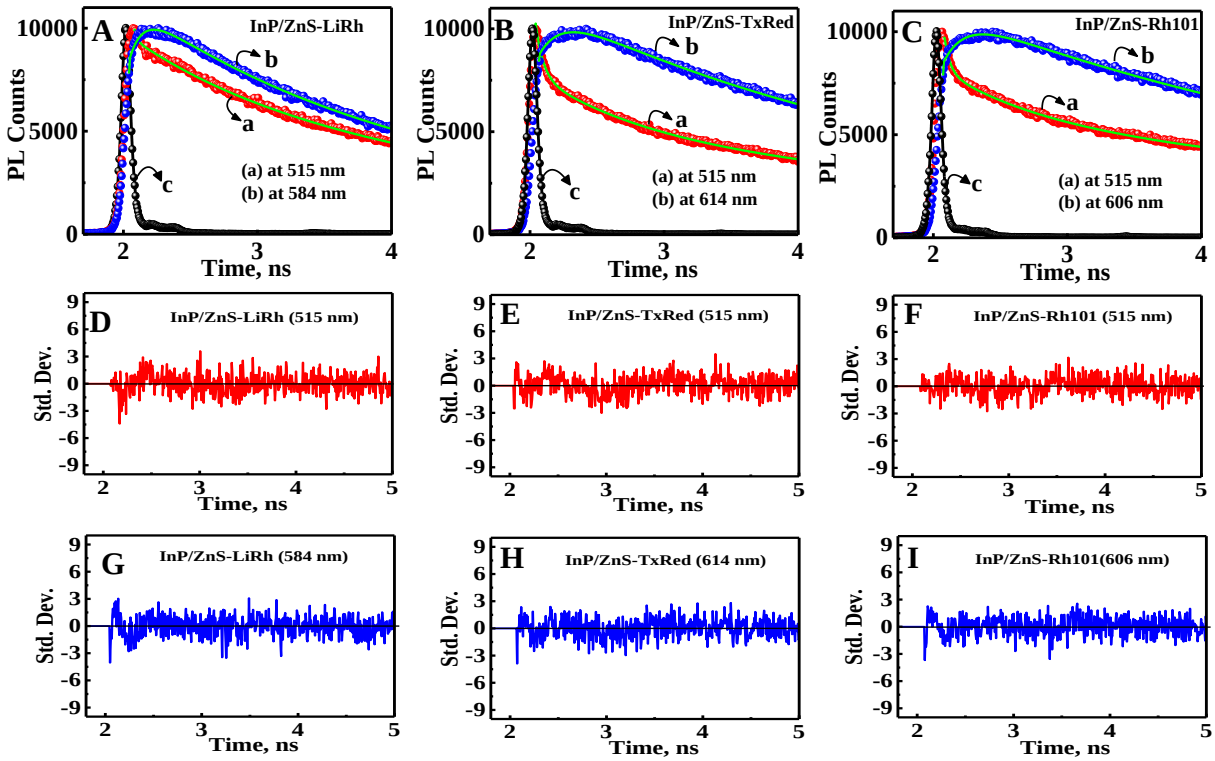

Figure S9. (A-C) Fitted luminescent decay curves of chromophore bound InP/ZnS monitored at 515 nm (red trace a) and at the corresponding emission maximum of chromophoric dyes (blue trace b in A-C): (A) InP/ZnS-LiRh, (B) InP/ZnS-TxRed and (C) InP/ZnS-Rh101. The solid line drawn through the decay curve in (A-C) shows the fitting. The lamp profile of the picosecond pulse is shown (black trace c in A-C). Residual plots of the fit corresponding to the decay collected (D-F) at 515 nm (red trace) and (G-I) at the emission maximum of the corresponding chromophoric dye (blue trace): (D,G) InP/ZnS-LiRh, (E,H) InP/ZnS-TxRed and (F,I) InP/ZnS-Rh101.

Table S3. Emission decay analysis of chromophore bound InP/ZnS measured in a time window of 50 ns

Sample	λ	τ_1 (ns)	α_1	τ_2 (ns)	α_2	τ_3 (ns)	α_3	τ_4 (ns)	α_4	Chi. Sq.
InP/ZnS-LiRh	514	3.92	0.35	12.80	0.05	1.18	0.18	0.02	0.42	1.03
	584	3.51	0.48	11.84	0.04	1.71	0.26	0.16	-0.22	1.04
InP/ZnS-TxRed	514	3.43	0.33	13.94	0.14	0.81	0.21	0.06	0.32	1.06
	614	4.18	0.65	13.75	0.05	1.84	0.10	0.19	-0.20	1.04
InP/ZnS-Rh101	514	3.17	0.32	17.77	0.24	0.71	0.18	0.05	0.26	1.00
	608	4.50	0.64	09.27	0.15	1.20	0.01	0.18	-0.20	1.01

λ = wavelength at which the emission is collected;

10. Energy transfer using InP/ZnS@530 and InP/ZnS@500

InP/ZnS quantum dots emitting at 530 nm (InP/ZnS@530) and 500 nm (InP/ZnS@500) were used to tune the overlap integral and investigate the energy transfer using LiRh and TxRed acceptors. The steady state and time resolved emission investigations confirm Förster energy transfer process. Concentration of the donor InP (0.66 μM) QDs and acceptor molecules, LiRh (0.25 μM) and TxRed (0.40 μM), were maintained as in the case of InP/ZnS emitting at 515 nm.

10.1. InP/ZnS@530 based donor acceptor system

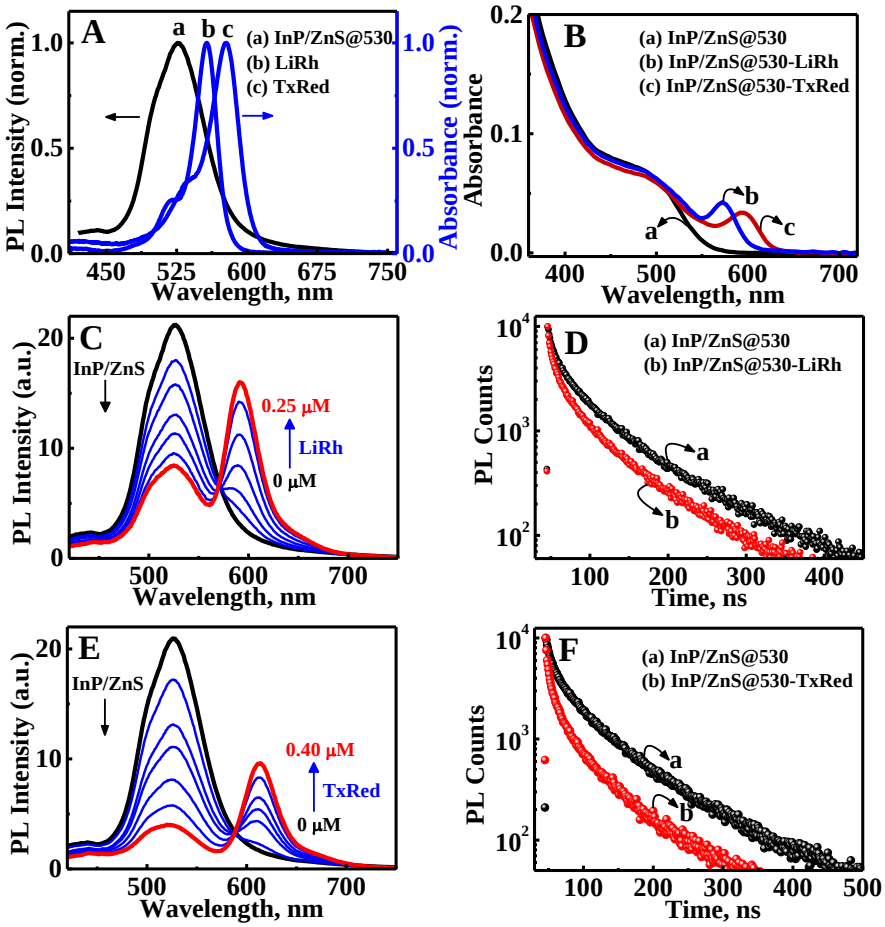

Figure S10. (A) The spectral overlap between the emission of InP/ZnS@530 (black trace a) and absorption of LiRh (blue trace b) and TxRed (blue trace c). (B) Absorption spectrum of InP/ZnS@530 (black trace a), InP/ZnS@530-LiRh (blue trace b) and InP/ZnS@530-TxRed (red trace c). (C, E) Steady state emission spectral changes of InP/ZnS@530 on addition of chromophoric dyes excited at 400 nm: (C) LiRh, (E) TxRed. (D,F) Luminescence decay profile of InP/ZnS@530 in the absence (black trace a in D, F) and presence of chromophoric dye represented by red trace b: (D) LiRh (0.25 μM), (F) TxRed (0.40 μM).

Table S4. Energy transfer parameters for chromophore bound InP/ZnS@530 system

Chromophore bound InP/ZnS@530	$J(\lambda)$ ($M^{-1}cm^{-1}nm^4$)	R_0 (Å)	E^a (%)	r (Å)	$k_T(r)$ (s^{-1})
InP/ZnS@530-LiRh	8.28 x 10^{15}	50.70	60.38	47.28	4.20 x10^7
InP/ZnS@530-TxRed	3.35 x 10^{15}	43.61	80.52	34.43	1.14 x10^8

R_0 = Förster distance, $J(\lambda)$ = overlap integral; E = efficiency calculated using [a]steady state data; r = distance between the donor and acceptor; $k_T(r)$ = rate of energy transfer.

10.2. InP/ZnS@500 based donor acceptor system

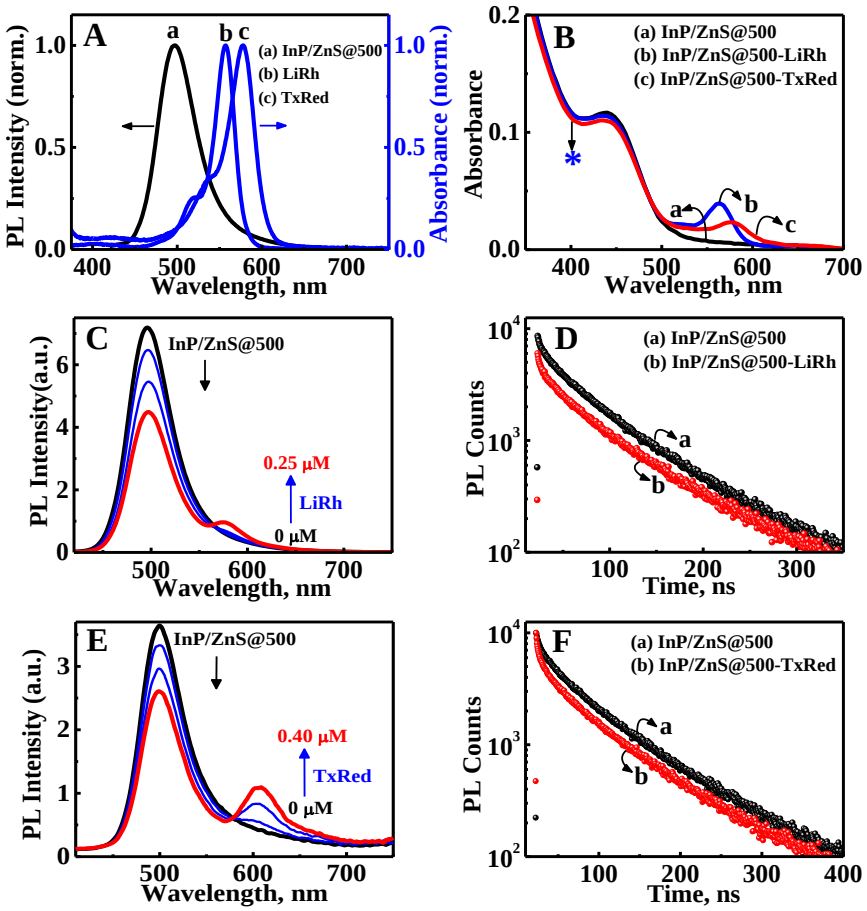

Figure S11. (A) The emission of InP/ZnS@500 (black trace a) and absorption of chromophoric dye showing spectral overlap: LiRh (blue trace b) and TxRed (blue trace c). (B) Absorption spectrum of InP/ZnS@500 (black trace a), InP/ZnS@500-LiRh (blue trace b) and InP/ZnS@500-TxRed (red trace c). (C,E) Steady state emission spectral changes of InP/ZnS@500 on addition of chromophoric dyes excited at 400 nm: (C) LiRh, (E) TxRed. (D,F) Luminescence decay profile of InP/ZnS@500 in the absence (black trace a in D, F) and presence of chromophoric dye represented by red trace b: (D) LiRh (0.25 μM), (F) TxRed (0.40 μM).

Table S5. Energy transfer parameters for chromophore bound InP/ZnS@500 system

Chromophore bound InP/ZnS@500	$J(\lambda)$ ($M^{-1}cm^{-1}nm^4$)	R_0 (Å)	E^a (%)	r (Å)	$k_T(r)$ (s^{-1})
InP/ZnS@500-LiRh	2.97 x 10^{15}	40.59	38.01	44.04	9.02 x10^6
InP/ZnS@500-TxRed	1.50 x 10^{15}	36.19	28.51	42.18	5.32 x10^6

R_0 = Förster distance, $J(\lambda)$ = overlap integral; E = efficiency calculated using [a]steady state data; r = distance between the donor and acceptor; $k_T(r)$ = rate of energy transfer.

11. Energy transfer in water soluble InP/ZnS Quantum dots

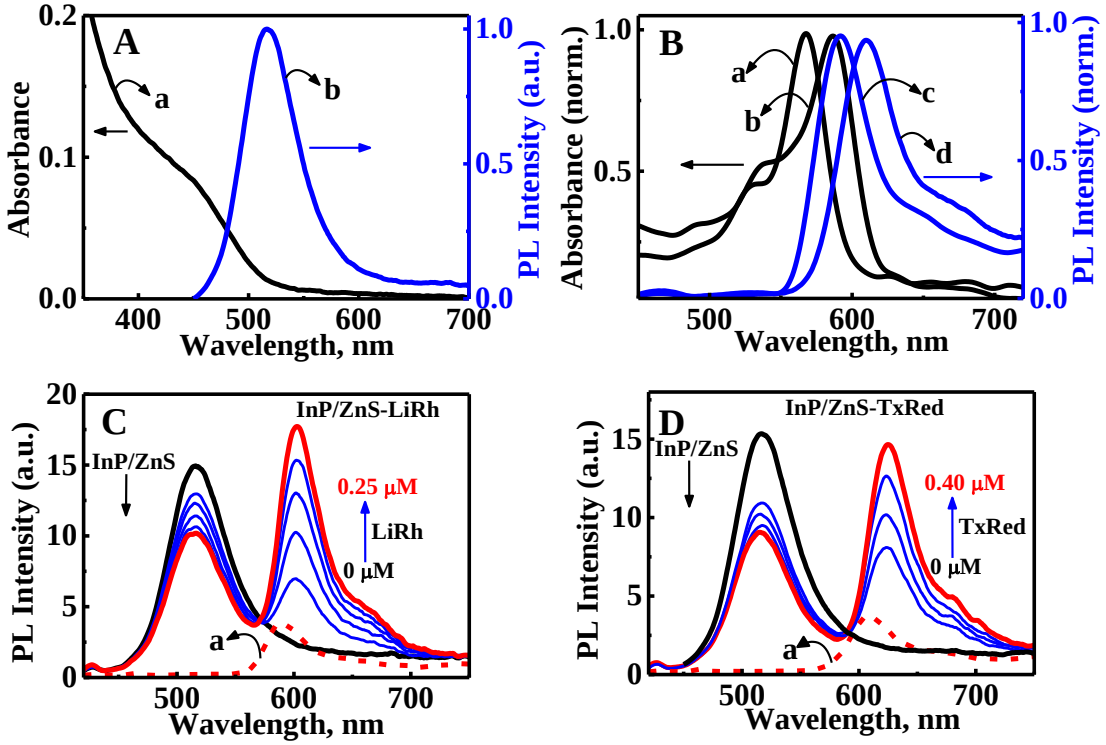

Figure S12. (A) Steady state absorption (black trace a) and emission (blue trace b) spectra of water soluble InP/ZnS quantum dots. (B) Absorption spectrum of LiRh (black trace a) and TxRed (black trace b) and corresponding emission spectrum of LiRh (blue trace c) and TxRed (blue trace d) in aqueous medium. (C,D) Steady state emission spectral changes of water soluble InP/ZnS on addition of chromophoric dyes (excited at 400 nm): (C) LiRh (0.25 μM), and (D) TxRed (0.40 μM). The red dashed trace a in (C) and (D) shows the emission spectrum of LiRh (0.25 μM) and TxRed (0.40 μM) in aqueous medium when excited at 400 nm in the absence of InP/ZnS quantum dots.

12. Reference

(1) Xie, R.; Battaglia, D.; Peng, X. Colloidal InP Nanocrystals as Efficient Emitters Covering Blue to Near-Infrared. *J. Am. Chem. Soc.* **2007,** *129,* 15432-15433.